- Technical Paper -

PULL OUT AND DIRECT TENSILE PROPERTIES OF FIBER REINFORCED CEMENTITIOUS COMPOSITES

Yaechan LEE[*1], Gyuyong KIM[*2], Byungcheol CHOI[*1] and Jeongsoo NAM[*2]

ABSTRACT

This study evaluated the effect of fiber on pull-out and tensile properties by conducting pull-out tests and direct tensile tests on hooked steel fiber (HSF), bundle-type polyamide fibers (PA), and amorphous metallic fibers (AF) with various physical properties and shapes. As a result, the hooked steel fiber was pulled-out, and the bonding stress and mechanical bonding stress of the fiber and the matrix had a great influence on the tensile performance. PA and AF showed fracture behavior, and the tensile performance of the fiber itself had a great influence on the tensile properties.

Keywords: direct tensile strength, pull-out, fiber, strain capacity, toughness

1. INTRODUCTION

Cement-based materials are used as main materials for buildings because of their excellent compressive strength and durability. However, due to its low flexural and tensile strength, it has brittle fracture properties, and to compensate, research on fiber reinforced cementitious composites that reinforce fiber in matrix is underway [1-2].

The fiber reinforced cementitious composites (FRCC) is a material that restrain cracks through the bridging reaction of fibers arranged discontinuously inside the matrix by incorporating single fiber into the matrix, thereby greatly improving flexural and tensile strength, strain capacity, fracture resistance performance, and load-holding ability [3-4].

When fracture occurs in such a fiber reinforced cementitious composites, the pull-out behavior of the fiber varies according to the shape and type of the fiber to be reinforced.

First, the fiber restrains cracks by bonding between the fiber and the matrix before cracks occur in the matrix. After cracks have occurred in the cement matrix, more cracks are restrained by bridging reaction due to bonding stress of the fiber and matrix, and strain hardening occurs in this process. After that, as the fracture progresses further, strain softening occurs, and fibers are pull-out or fracture depending on various factors, and this behavior affects the tensile properties of the cementitious composites, and studies related to this pull-out behavior are being conducted [5].

As such, it is reported that the pull-out behavior of fibers varies depending on the shape and physical properties of fibers and affects mechanical properties of fiber reinforced cementitious composites such as flexural and tensile strength

However, in the case of hooked steel fiber that have been previously used, it is difficult to use due to the specific gravity of the fiber itself and corrosion. Therefore, it is necessary to check the possibility of use in cement-based materials by selecting fibers having different shapes and physical properties from the same length.

Therefore, in this study, the effect of fiber pull-out behavior on the tensile properties of the cementitious composites was analyzed and the correlation of the factors affecting it was analyzed by conducting a pull-out test of hooked steel fibers, polyamide fibers, and amorphous metallic fiber with different shapes and properties.

2. TEST PROGRAMS

2.1 Experimental plan

Table 1 shows the details of specimen of this study, and the fibers were hooked steel fiber (HSF), bundle-type polyamide fiber (PA), and amorphous metallic fiber (AF), which were reinforced with 1.0 and 2.0 vol%, respectively.

2.2 Materials and mix proportion

Table 2 and Fig. 1 show the mechanical properties and shape of the fiber. The hooked steel fiber is cylindrical, has a diameter of 0.5 mm, a specific surface of 1.0 m^2/kg, a tensile strength of 1,140 MPa, and both ends of the fiber are bent in a hook shape. The bundle-type polyamide fiber is a fiber formed by air injection of 544 fine short fibers having a diameter of 19.5 μm, and has a diameter of 0.5 mm, a specific surface area of 15.6 to 329.9 m^2/kg, and a tensile strength of 594 MPa. The amorphous metallic fiber has a thin plate shape, a width of 1.6 mm, a thickness of 29 μm, a speci fic surface area of 9.6 m^2/kg, and a tensile strength of 1,400 MPa.

*1 Doctoral Course, Dept. of Architecture Engineering, Chungnam National University, JCI Member
*2 Prof., Dept. of Architecture Engineering, Chungnam National University, JCI Member

Table 1 Experimental plan

ID.	Type of fiber	Fiber volume fraction
HSFRCC 1.0	Hooked	1.0 vol.%
HSFRCC 2.0	steel fiber	2.0 vol.%
PARCC 1.0	Bundle-type	1.0 vol.%
PARCC 2.0	polyamide fiber	2.0 vol.%
AFRCC 1.0	Amorphous	1.0 vol.%
AFRCC 2.0	metallic fiber	2.0 vol.%

Table 2 The mechanical properties of fiber

Type	HSF	PA	AF
Length (mm)	30	30	30
Diameter (mm)	0.5	0.5	0.25*1
Width (mm)	-	-	1.6
Thickness (μm)	-	-	29
Density (g/cm3)	7.85	1.14	7.2
Specific surface area (m2/kg)	1.0	15.6~329.9	9.6
Tensile strength (MPa)	1,140	597	1,400
Aspect ratio(L/D)	60	60	120
The number of fiber (/kg)	22,000	330,000	100,000

*1: Equivalent diameter

(a) HSF (b) PA (c) AF

Fig.1 Used fibers

Table 4 Mix proportion

W/B	Unit weight (Kg/m^3)				Fiber		
	Cement	Water	Fly -ash	Silica sand	Type	Vol.%	kg
0.4	850	400	150	350	HSF	1.0	78.5
						2.0	157
					PA	1.0	11.4
						2.0	22.8
					AF	1.0	72
						2.0	114

The length of the fiber used is the same as 30 mm, but the diameter of the hooked steel fiber and the bundle-type polyamide fiber is 0.5 mm, the aspect ratio of the amorphous steel fiber is 0.25 mm, and the aspect ratio by the same diameter is 120. Originally, it is reasonable to compare the mechanical properties of the used material equally, but since amorphous metallic fibers have a unique thin plate shape, it was necessary to compare their performance with fibers of the same length even with different aspect ratio.

Table 3 shows the mix proportion of cementitious composites. In order to satisfy the target of compressive strength, W/B was set to 0.4. In addition, fly ash and type 7 silica sand were used to secure the dispersibility of fibers and warkability.

2.3 Experimental method

Fig. 2 shows the shape of the fiber drawing test

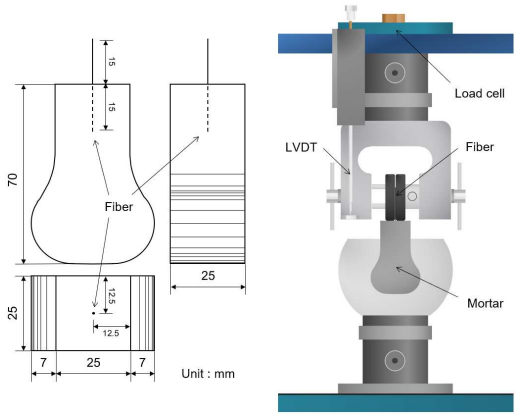

(a) Shape of specimen (b) Equipment of pull-out test

Fig.2 Pull-out test set up

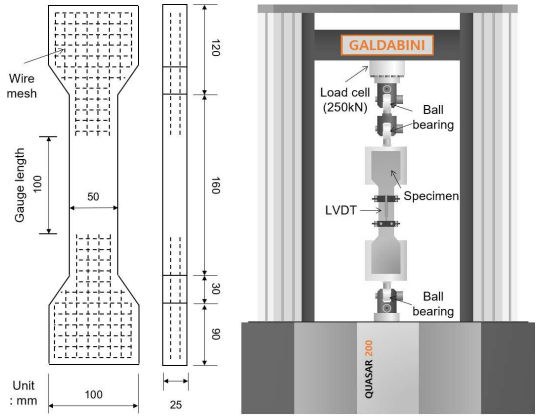

(a) Shape of specimen (b) Equipment of tensile test

Fig.3 Tensile test set up

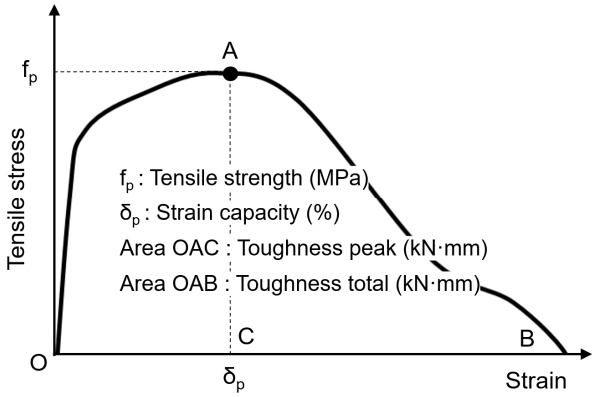

Fig.4 Summary of tensile properties

specimen and the fiber pull-out test device [6]. As shown in the shape of the specimen, 15 mm, half of the fiber, was embeded in the center of the specimen 25 mm x 25 mm to conduct a pull-out test, and the pulled hooked steel fiber was calculated as shown in Equation (1), and the fracture bundle-type polyamide fiber and amorphous metallic fiber were calculated as shown in Equation (2).

$$\tau_{max} = P_{max}/\pi DL \quad (1)$$

$$\sigma_{max} = P_{max}/A \quad (2)$$

Where,

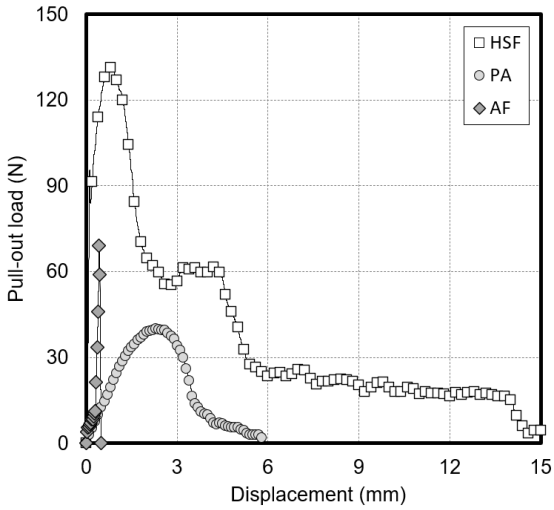

Fig.5 Pull-out load-displacement curve

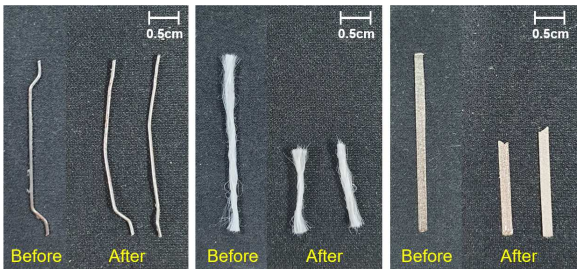

Fig.6 Fiber shape after pull-out test

Table 4 Pull-out data

Type	Peak load (N)	Displacement at peak load (mm)	Pull-out toughness (N·mm)	τ_{max}	σ_{max}
HSF	131.90	0.73	571.32	5.60	671.76
PA	40.20	2.51	113.08	1.71	204.74
AF	69.25	0.43	9.35	1.42	1492.46

τ_{max} : The fiber pull-out strength (MPa)
σ_{max} : The fiber fracture strength (MPa)
P_{max} : The maximum pull-out load (N)
D : The diameter of the fiber (mm)
L : The embedded length of the fiber (mm)
A : The cross section of the fiber (mm^2)

Fig. 3 shows the shape of the tensile test specimen and the direct tensile test device. The tensile strength test specimen is in the form of a dogbone, with a size of 400 mm × 100 mm × 25 mm (length × width × thickness) and a cross section of the central part of the test specimen being 25 mm × 50 mm (width × length). In order to prevent cracks in the neck area where there is a change in the cross-section of the test specimen, the wire mesh was reinforced to induce cracks within the target distance. The test was conducted using a 250 kN direct tensile test device, the loading speed was about 1 mm/min, and the strain of the test specimen was measured by installing a jig with LVDT attached to the test specimen.

Fig. 4 shows the tensile stress-strain curve summarizing the tensile performance. To evaluate tensile performance in this test, tensile strength (maximum stress point), strain capacity (strain at maximum stress), peak toughness (area of tensile stress-strain curve to maximum force point), and overall toughness (area of tensile stress-strain curve until final destruction of the test specimen) were derived.

3. RESULTS AND DISCUSSION

3.1 Properties of pull-out test

The pull-out load-displacement curve in Fig. 5, the shape of the fiber after the pull-out test in Fig. 6, and the pull-out test data in Table 4 are shown.

Hooked steel fiber showed pull-out behavior after the maximum load, and the pull-out load tended to gradually decrease after the peak due to the pull-out as the hooked-shape at the end of the fiber gradually unfolded during the pull-out process.

On the other hand, the bundle-type polyamide fiber showed a behavior in which the fiber increased by 2.5 mm to the maximum load and then fracture after the maximum load due to the high elongation. This is considered to be fractured because the bonding stress between the fiber and the matrix is higher than the tensile strength of the fiber itself.

Amorphous metallic fiber has a rough surface and a large bonding area between the fiber and the matrix, resulting in a fracture because they have higher bonding strength than the tensile strength of the fiber itself. Amorphous metal is known to have high toughness, but amorphous metallic fiber is thin in the form of thin plates, so it is judged that the load that can withstand is not high. Because of the fracture behavior of the fiber, it was determined that the amorphous metallic fiber had a higher effect on the bonding stress of the fiber and the matrix than the tensile strength [7].

Through the fiber pull-out test, it was confirmed that the pull-out behavior, pull-out strength, and fracture strength differed significantly depending on the shape and physical properties of the fiber, and accordingly, it was considered that it was necessary to compare it in conjunction with the pull-out behavior of the fiber during the direct tensile test.

3.2 Properties of direct tensile test

Fig. 7 shows the tensile stress-strain curve of the cementitious composite, and Fig. 8 shows the fiber pull-out and fracture photographs after the direct tensile test according to the type of fiber.

In the case of HSFRCC, strain hardening behavior due to bridging reaction of fiber after initial cracking was shown. In addition, during the direct tensile test, it was confirmed that the hooked steel fiber was pull-out from the matrix, and when it was pull-out, the hook-shape at the end of the fiber was straightened and slowly pulled out. For this reason, it is determined that the stress in the stress-strain curve gradually decreases after the peak.

In the case of PAFRCC, as in the pull-out test, the bundle-type polyamide fibers bonded to the matrix and stretched and fracture, and in this process, the stress decreased and increased repeatedly arose from In addition, although the tensile strength is smaller than that

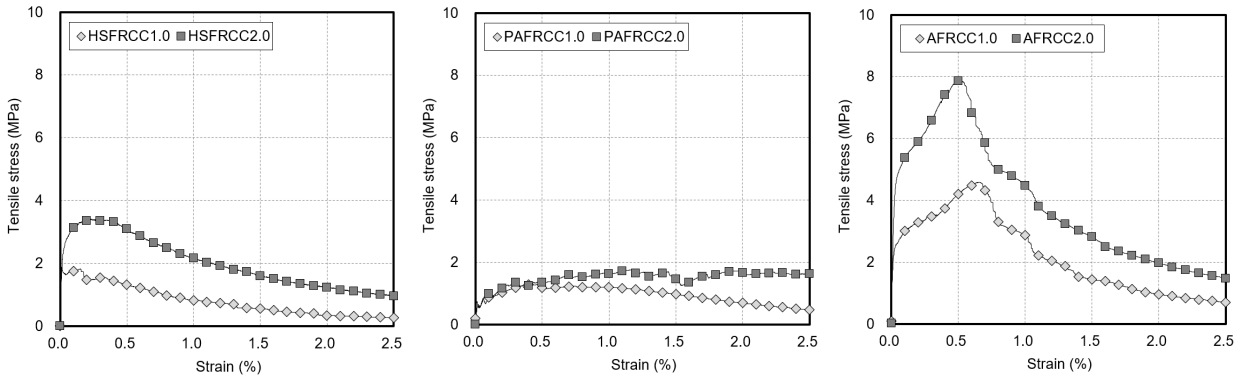

(a) HSFRCC (b) PAFRCC (c) AFRCC

Fig.7 Tensile stress-strain curve

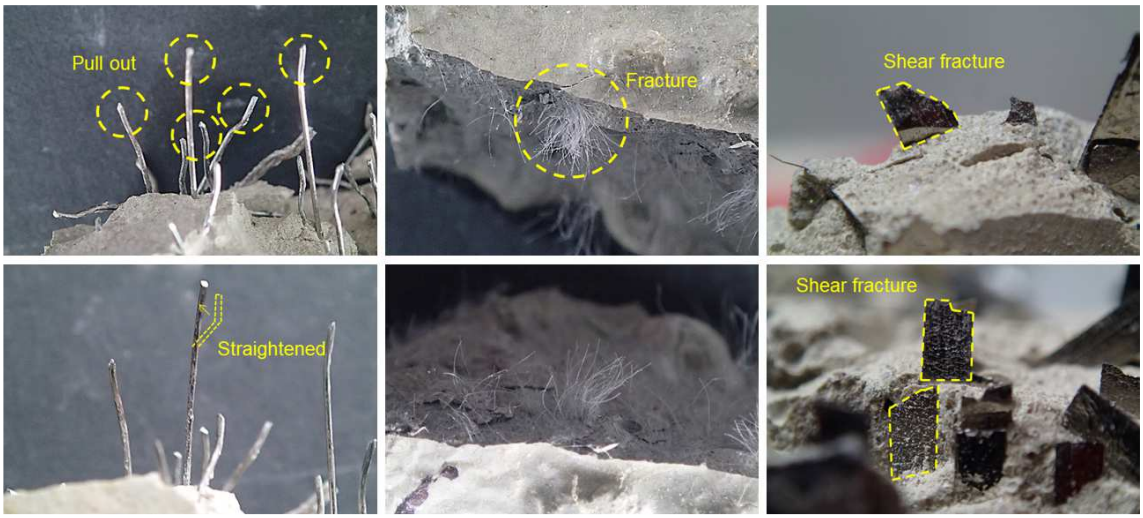

(a) HSF (b) PA (c) AF

Fig.8 Shape of fiber after direct tensile test

of other specimens, the elongation of the fiber is high, and the number of fibers per unit volume is large, so the tensile stress is smoothly dispersed and the strain capacity is excellent [8].

In the case of AFRCC, it was confirmed that the strain hardening behavior was clearly observed due to the bridging reaction of the fiber after the initial crack. In addition, the bonding stress with the matrix and fiber was excellent due to the large bonding area of the fiber, and the tensile strength was measured higher than that of other specimens due to the large number of fibers per unit volume. However, due to the properties of amorphous metallic fiber that are vulnerable to shear force and brittlely fractured, fiber fracture after maximum stress was observed, and the stress tends to decrease rapidly compared to other test specimens.

Fig. 9 shows the data values for the tensile strength, strain capacity, and toughness of the test specimen in a graph. In the case of AFRCC, the tensile strength was excellent because the bonding strength of amorphous metallic fiber was high and the number of fiber mixed was large. PAFRCC is greatly affected by the tensile performance of the fiber itself due to the fracture behavior of the fiber, and as a result, the tensile strength of the bundle-type polyamide fiber itself is low, so it is considered that the tensile strength is lower than that of other tests.

In the case of strain capacity, PAFRCC showed the best strain capacity due to its high stress dispersing ability, as the elongation of bundle-type polyamide fibers is high and a large number of fibers per unit volume are reinforced. Comparing AFRCC and HSFRCC, the number of fibers of amorphous metallic is higher than that of hooked steel fiber, so the binding force by fiber bonding stress is high along with stress dispersion caused according to many cracks.

Toughness represents the energy required for specimen deformation, and the peak toughness and the overall toughness are calculated by the area of the tensile stress-strain curve, which is closely related to the tensile strength and strain ability. AFRCC has excellent tensile strength, so it is considered that its peak toughness and overall toughness were higher than those of other specimens. HSFRCC was evaluated to have low peak toughness due to its low strain capacity, but its overall toughness slightly increased due to its excellent load-holding ability due to the pull-out behavior of fiber. In the case of PAFRCC, the strain capacity was high but the tensile strength was low, so the peak toughness and the overall toughness were measured lower than that of AFRCC.

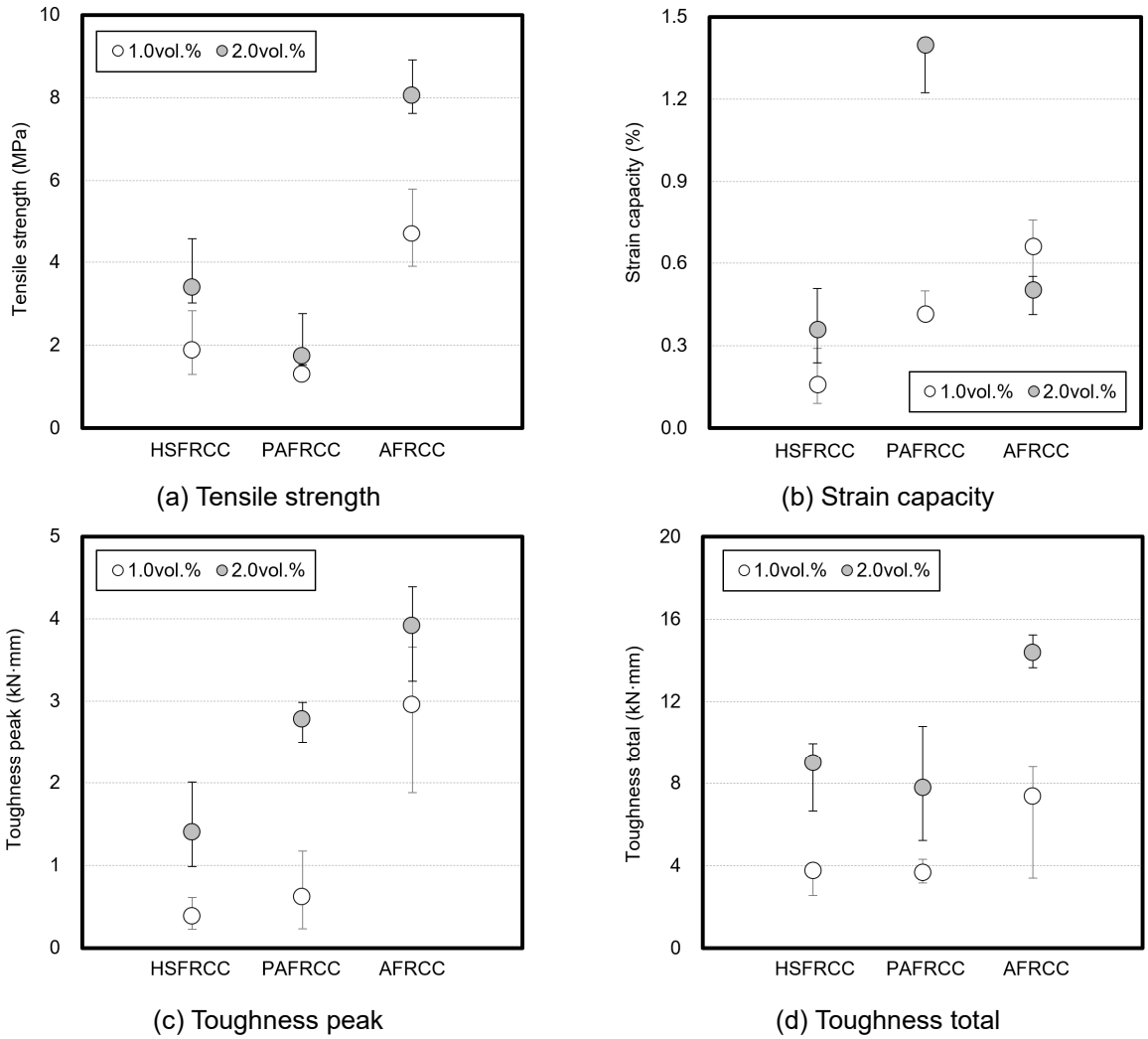

(a) Tensile strength (b) Strain capacity

(c) Toughness peak (d) Toughness total

Fig.9 Tensile properties

3.3 Relationship between Pull-out behavior and tensile properties

Fig. 10 shows a schematic diagram of the fiber pull-out behavior according to the tensile stress-strain curve. The elastic section, the strain hardening section, and the strain softening section were divided into three sections, and the behavior of fibers that are considered to have a relatively large influence in each section was expressed. All types of fibers are attached to the matrix in the elastic section to restrain cracks, and after the initial cracks, a change in pull-out behavior occurs.

In the case of HSF, a part of the matrix is removed from the fiber in the strain hardening section along with the initial crack, but the bridging reaction of the fiber and matrix restrains the crack, and the hook at the end of the fiber appears to be pull-out in the strain softening section. Due to the pull-out behavior of such fibers, it is considered that mechanical bonding stress by the bonding stress of the hooked steel fiber and the matrix and the fiber shape greatly affects the tensile performance of the cementitious composites.

In the case of PA, the fibers stretch and fracture after initial cracking, which led to repeated curves of strain hardening and softening, unlike other fibers. Due to the fracture behavior of the fiber, it is considered that the tensile performance of the fiber itself greatly affects that of the cementitious composites.

In the case of AF, the matrix and fiber are partially separated in the strain hardening section with the initial crack, but the bridging reaction of the fiber between the cracks restrains the crack in the matrix, and the fiber appears to be fractured in the strain softening section. Due to the fracture behavior of the fiber, it is judged that the tensile performance of the fiber itself greatly affects that of the cementitious composites.

4. CONCLUSIONS

The following conclusions were obtained from a fiber pull-out test of hooked steel fiber, bundle-type polyamide fiber, and amorphous metallic fiber, and a direct tensile test of a cementitious composites reinforced with fiber.

(1) Hooked steel fiber tended to be pull-out as the hook-shape at the end of the fiber was straightened, and as a result, they showed high load-holding ability. In addition, it is judged that the bonding stress and mechanical bonding stress of the fiber and the matrix have a great influence on the tensile performance of HSFRCC by showing the pull-out behavior without fiber fracture.

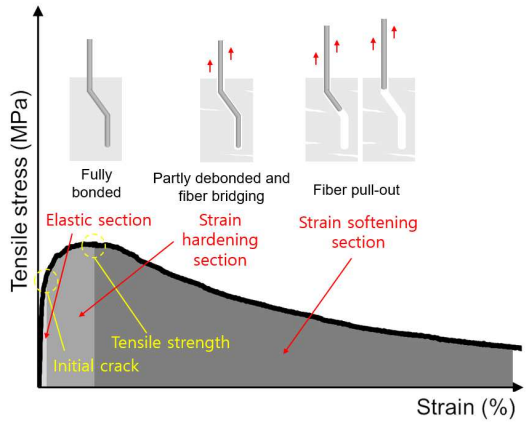

(a) HSFRCC

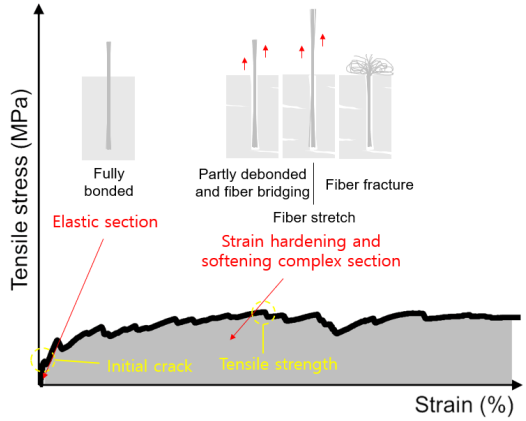

(b) PARCC

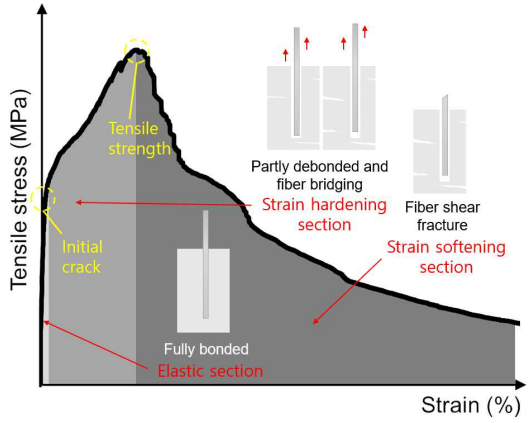

(c) AFRCC

Fig.10 The schematic diagram between fiber and tensile properties

(2) As a bundle-type polyamide fiber fractures, fiber itself tensile performance greatly affects the tensile performance of PAFRCC and its strain capacity is greatly improved due to its high elongation and excellent stress dispersing ability.

(3) The tensile strength of amorphous metallic fibers was higher than other FRCCs due to their large population, rough surface, and wide bonding area, but the fiber was fractured due to its weak shear force due to the thin plate shape. In addition, it is judged that the tensile performance of the fiber itself greatly affects the tensile performance of AFRCC due to the fracture behavior of the fiber.

(4) Based on this study, the tensile strength of FRCC depends on the pull-out strength and fracture strength of the pull-out characteristics along with the fiber mixing population, and this pull-out and fracture strength are affected by the specific surface area and tensile strength of the fiber. In addition, the strain capacity of FRCC is due to fiber mixing population and pull-out deformation, and this pull-out deformation seems to be closely related to fiber elongation and specific surface area. Through this, it is judged that various factors affecting the tensile performance of the cement composite have a complex interaction.

ACKNOWLEDGEMENT

This work was supported by the National Research Foundation of Korea(NRF) grant funded by the Korea government(MSIT). (No. 2019R1A2C2085867)

REFERENCES

[1] Qiao, D., Honma, D., & Kojima, M (2019). Evaluation of tensile behavior of ultra high performance fiber reinforced concrete with uniaxial tension tests. Proceedings of the Japan Concrete Institute, 41(1), 323-328.

[2] Kim, H., Kim, G., Gucunski, N., Nam, J., & Jeon, J. (2015). Assessment of flexural toughness and impact resistance of bundle-type polyamide fiber-reinforced concrete. Composites Part B: Engineering, 78, 431-446.

[3] Jeong, G. Y., Jang, S. J., Kim, Y. C., & Yun, H. D. (2018). Effects of steel fiber strength and aspect ratio on mechanical properties of high-strength concrete. J. Korea Conc. Inst, 30, 197-206.

[4] Lee, S., Kim, G., Kim, H., Son, M., Choe, G., & Nam, J. (2018). Strain behavior of concrete panels subjected to different nose shapes of projectile impact. Materials, 11(3), 409.

[5] Jamshidi, M., & Karimi, M. (2010). Characterization of polymeric fibers as reinforcements of cement‐based composites. Journal of applied polymer science, 115(5), 2779-2785.

[6] Kang, S. H., Kim, J. J., Kim, D. J., & Chung, Y. S. (2013). Effect of sand grain size and sand-to-cement ratio on the interfacial bond strength of steel fibers embedded in mortars. Construction and Building materials, 47, 1421-1430.

[7] Kim, H., Kim, G., Lee, S., Choe, G., Nam, J., Noguchi, T., & Mechtcherine, V. (2020). Effects of strain rate on the tensile behavior of cementitious composites made with amorphous metallic fiber. Cement and Concrete Composites, 108, 103519.

[8] Kim, H., Kim, G., Lee, S., Son, M., Choe, G., & Nam, J. (2019). Strain rate effects on the compressive and tensile behavior of bundle-type polyamide fiber-reinforced cementitious composites. Composites Part B: Engineering, 160, 50-65.